Epidemic plateau in critical susceptible-infected-removed dynamics with nontrivial initial conditions

Filippo Radicchi[1] and Ginestra Bianconi[2,3]

[1]*Center for Complex Networks and Systems Research, Luddy School of Informatics, Computing, and Engineering, Indiana University, Bloomington, Indiana 47408, USA*

[2]*The Alan Turing Institute, 96 Euston Rd, London NW1 2DB, United Kingdom*

[3]*School of Mathematical Sciences, Queen Mary University of London, London E1 4NS, United Kingdom*

(Received 29 July 2020; accepted 18 October 2020; published 12 November 2020)

Containment measures implemented by some countries to suppress the spread of COVID-19 have resulted in a slowdown of the epidemic characterized by time series of daily infections plateauing over extended periods of time. We prove that such a dynamical pattern is compatible with critical susceptible-infected-removed (SIR) dynamics. In traditional analyses of the critical SIR model, the critical dynamical regime is started from a single infected node. The application of containment measures to an ongoing epidemic, however, has the effect to make the system enter in its critical regime with a number of infected individuals potentially large. We describe how such nontrivial starting conditions affect the critical behavior of the SIR model. We perform a theoretical and large-scale numerical investigation of the model. We show that the expected outbreak size is an increasing function of the initial number of infected individuals, while the expected duration of the outbreak is a nonmonotonic function of the initial number of infected individuals. Also, we precisely characterize the magnitude of the fluctuations associated with the size and duration of the outbreak in critical SIR dynamics with nontrivial initial conditions. Far from herd immunity, fluctuations are much larger than average values, thus indicating that predictions of plateauing time series may be particularly challenging.

DOI: 10.1103/PhysRevE.102.052309

I. INTRODUCTION

At the onset of the COVID-19 pandemic, worldwide time series of the number of infected individuals have displayed an exponential growth. Such a behavior is well predicted by standard epidemic frameworks [1]. In slightly later stages, however, time series have exhibited nontrivial dynamical patterns. Many papers have attempted to model observed behaviors and to determine the role of containment measures [2–17]. The common and reasonable assumption is that containment measures implemented in the attempt of mitigating the outbreak have strongly influenced the unfolding of the epidemic. Unfortunately, this a setting where modeling attempts are particularly challenging. The effective implementation of containment measures imposed by authorities relies on people's personal judgments and adaptive behavior, and while epidemic spreading is a well-studied branch of mathematical biology [18], statistical physics [19], and network science [20–26], the modeling of adaptive behavior is only at its infancy [27–29].

According to the data, in several countries, the slowdown of the epidemic spread is characterized by an almost flat time series of daily number of new infections. Moreover, the time series of the number of removed individuals display power-law growth instead of an exponential growth as a function of time [12,14,16,17]. Here, we propose a theoretical interpretation of those features as the signature of the system being in (or near) its critical regime. Criticality is a fundamental property characterizing the dynamics of biological and sociotechnical systems [30–32]. Our work consists of an in-depth investigation of a critical susceptible-infected-removed (SIR) dynamics starting from a nontrivial initial configuration characterized by n_0 initially infected individuals. We interpret the emergence of the critical regime as the result of disease containment strategies, and the nontrivial initial condition as the configuration of the system when spreading becomes critical. In the typical setting considered in statistical mechanics [33–35], a single seed is generally used as the initial condition for critical SIR dynamics; the mapping of the critical SIR to the critical standard branching process allows for a full characterization of the spreading dynamics [36,37]. The realistic assumption of having an initial number of infected individuals $n_0 > 1$ introduces an additional scale in the system affecting in a nontrivial manner the scaling properties of the SIR critical dynamics. While in other nonequilibrium systems a nontrivial initial condition may lead to a change of the critical exponent values [38–40], in the critical SIR, the introduction of a nontrivial initial condition does not change the critical exponents that characterize the distribution of outbreak size and duration. However, it introduces lower exponential cutoffs in the distributions. As a result, the expected size and duration of the outbreak, as well as their standard deviations, have a nontrivial dependence on the initial condition n_0. In this paper, we evaluate, by means of analytic arguments and large-scale simulations, the scaling of these quantities as functions of the population size N.

The paper is structured as follows: In Sec. II, we provide the theoretical interpretation of the plateau as a critical SIR

dynamics starting from $n_0 > 1$ initial condition; in Sec. III, we perform a statistical mechanics investigation of the statistical properties of the critical SIR dynamics with nontrivial initial conditions, supported by extensive numerical simulations of the process; finally, in Sec. IV, we provide concluding remarks. The Appendix describes the Gillespie algorithm used in this work to simulate the critical SIR dynamics.

II. THEORETICAL INTERPRETATION OF THE PLATEAU

We consider the susceptible-infected-removed (SIR) model on a well-mixed population [19–26]. At any point in time, individuals can be found in three possible states: susceptible, infected, and removed. Susceptible individuals do not carry the disease but they can be infected; infected individuals carry the disease, and they can spread it to susceptible individuals; removed individuals are either removed or deceased, and they do not participate in the spreading dynamics. We indicate with λ the rate of infection, i.e., the expected number of spreading events occurring per unit of time. Without loss of generality, we set the recovery rate equal to one.

We start our discussion by focusing on the deterministic treatment of the SIR model on a well-mixed population with infinite size. If we indicate with s, i, and r the fractions of susceptible, infected, and removed individuals, respectively, we can write

$$\begin{aligned} \frac{ds}{dt} &= -\lambda si, \\ \frac{di}{dt} &= \lambda si - i, \\ \frac{dr}{dt} &= i. \end{aligned} \tag{1}$$

Please note that $s + i + r = 1$. The critical dynamical regime is characterized by

$$\lambda_c = 1. \tag{2}$$

If we start from an initial condition consisting of a fraction $i(0)$ of infected individuals and a fraction $r(0) = 0$ of removed individuals, at the onset of the epidemic, i.e., $t \ll 1$, we observe a different behavior depending on the value of λ. In the noncritical regime, i.e., $\lambda \neq \lambda_c$, the deterministic equations for i and r read as

$$\begin{aligned} \frac{di}{dt} &= \lambda si - i \simeq (\lambda - 1)i, \\ \frac{dr}{dt} &= i. \end{aligned} \tag{3}$$

Solutions of the above equations are

$$\begin{aligned} i(t) &= i(0)e^{(\lambda-1)t}, \\ r(t) &= \frac{i(0)}{\lambda - 1}e^{(\lambda-1)t}. \end{aligned} \tag{4}$$

In essence, in the subcritical regime, i.e., $\lambda < \lambda_c$, the number of infected individuals decays exponentially fast, and the number of removed individuals remains vanishing. In the supercritical regime, i.e., $\lambda > \lambda_c$, the number of infected and removed individuals displays an exponential increase. At criticality, i.e., $\lambda = \lambda_c$, the deterministic equations for i and r are

$$\begin{aligned} \frac{di}{dt} &= (s - 1)i \ll 1, \\ \frac{dr}{dt} &= i, \end{aligned} \tag{5}$$

leading to

$$\begin{aligned} i(t) &\simeq i(0), \\ r(t) &\simeq i(0)t. \end{aligned} \tag{6}$$

Therefore, according to the deterministic approach, for small times we should expect that the number of removed individuals at criticality increases linearly in time with a slope that is given by the initial condition $i(0)$, at the onset of the epidemics.

From the deterministic Eqs. (1), it is evident that

$$\frac{di}{ds} = -1 + \frac{1}{\lambda s}. \tag{7}$$

The equation can be integrated to obtain the well-known solution [19]

$$s(t) + i(t) - \frac{1}{\lambda}\ln s(t) = s(0) + i(0) - \frac{1}{\lambda}\ln s(0). \tag{8}$$

Using Eqs. (1), we can express the logarithmic derivative of the number of infected individuals as

$$\frac{d\,\ln i}{dt} = \lambda s - 1, \tag{9}$$

where $\lambda\, s(t)$ is the reproduction number. The former equation implies that the time series of infected individuals $i(t)$ has a peak at $t = t^\star$ determined by

$$\lambda s(t^\star) = 1. \tag{10}$$

The fraction of susceptible individuals at the peak of the epidemic is given by $s^\star = s(t^\star) = 1/\lambda$. By making the further assumption that the epidemic starts from a fraction $i(0) = 1 - s(0)$ of infected individuals and zero removed individuals $r(0) = 0$ in Eq. (8), we obtain

$$i^\star = i(t^\star) = 1 - \frac{1}{\lambda} - \frac{1}{\lambda}\ln[\lambda s(0)]. \tag{11}$$

Using Eqs. (10) and (11) in the first of Eqs. (1), we get

$$\left.\frac{ds}{dt}\right|_{t=t^\star} = -\lambda s^\star i^\star = -i^\star. \tag{12}$$

It follows that the second derivative of $\ln i$ is given by

$$\left.\frac{d^2 i}{dt^2}\right|_{t=t^\star} = i(t^\star)\left.\frac{d^2 \ln i}{dt^2}\right|_{t=t^\star} = -\lambda(i^\star)^2 = -\rho^\star, \tag{13}$$

where $\rho^\star$ is defined as

$$\rho^\star = -\frac{1}{\lambda}\{\lambda - 1 - \ln[\lambda s(0)]\}^2. \tag{14}$$

We note that $\rho^\star$ is zero, i.e., we reach a plateau, only for $s(0) = 1$ and $\lambda = 1$. This fact implies that, in the deterministic approach, a perfect plateau of the time series $\ln i$ is never achieved for $\lambda > 1$.

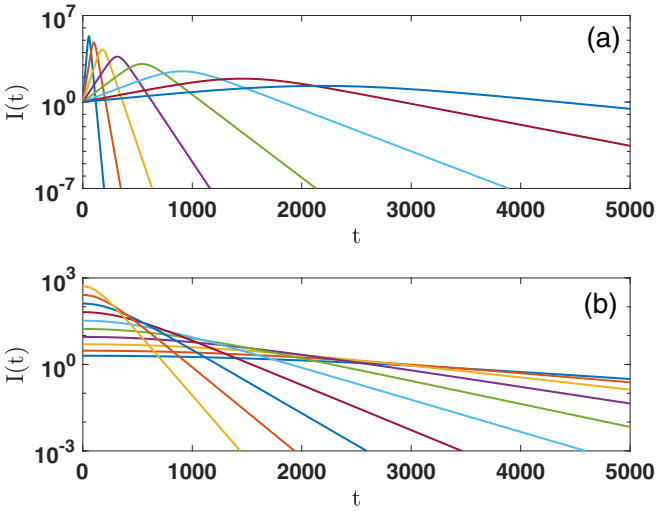

FIG. 1. (a) Time series of the number of infected individuals $I(t) = i(t)N$ are plotted close to the critical point. $I(t)$ correspond to the solution of the deterministic SIR equations. The population size is $N = 10^7$, and spreading is started from $n_0 = 1$ seed. Different curves correspond to different values of $\lambda = 1 + 2^{-q}$, with $q = 2, 3, 4, \ldots, 8, 9$. (b) Same as in (a), but for $\lambda = 1$. Different curves correspond to different numbers of initially infected nodes $n_0 = 2^q$, with $q = 2, 3, 4, \ldots, 8, 9$. As λ approaches the critical value $\lambda_c = 1$ and n_0 decreases toward one, we observe a plateauing of the time series.

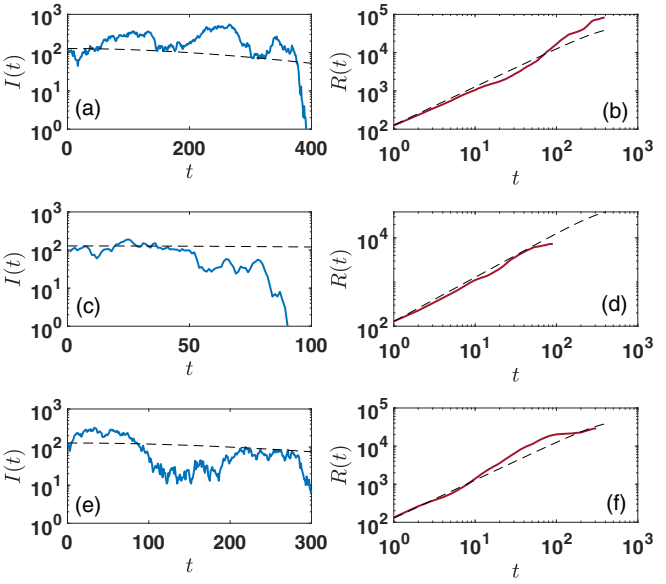

FIG. 2. We show three examples of time series for the number of infected individuals $I(t)$ [panels (a), (c), and (e)] and the corresponding number of removed individuals $R(t)$ [panels (b), (d), and (f)] for a critical SIR dynamics with nontrivial initial condition. The time series are obtained by simulating the stochastic SIR dynamics at criticality (with $\lambda = 1$) on a well-mixed population with identical parameters: initial number of infected individuals $n_0 = 128$ and population size $N = 10^7$. The dashed lines indicate the corresponding deterministic predictions.

In the vicinity of the critical point, the time series of the infected individuals is still well described by a plateau. Developing the right-hand side of Eq. (13) around $\lambda = 1$, $s(0) = 1$, we get $s(0) \simeq 1$ and

$$\rho^\star \simeq -\frac{1}{\lambda}\left[\ln[s(0)] + \frac{1}{2}(\lambda - 1)^2\right]^2 \simeq \left[1 - s(0) + \frac{1}{2}(\lambda - 1)^2\right]^2. \quad (15)$$

The above equation indicates that the conditions to have a near-plateau dynamics are having an infectivity rate λ close to one, and having the system as far as possible from herd immunity, i.e., $1 - s(0) \ll 1$. In summary, the near-critical state for $\lambda \simeq 1$ is a fragile state that can be characterized by a very slow dynamics if containment measures do not further decrease the infectivity λ below one (see Fig. 1).

III. SIR CRITICAL DYNAMICS WITH NONTRIVIAL INITIAL CONDITION

From now on, we assume that the system is in the critical regime. We further assume that spreading dynamics is started from $n_0 > 1$ initial seeds. The two assumptions serve to rationalize two main features of real time series. First, time series are characterized by long temporal windows of almost flat behavior. This is a signature of criticality. Second, plateaus are observed only after initial growths in the number of infected individuals, meaning that the critical regime is reached only after that containment strategies have effectively changed the spreading dynamics of the disease. Whereas critical properties of the SIR model are well understood for spreading processes initiated by $n_0 = 1$ individual, we are not aware of existing studies dealing with nontrivial initial conditions consisting of $n_0 > 1$ seeds. How do the properties of the critical dynamics change with n_0? What is the behavior of the expected duration of the outbreak? What about the expected size of the outbreak? What about their fluctuations?

Please note that all the above questions cannot be answered with a purely deterministic approach. SIR outbreak sizes and durations obey probability distributions that are well peaked around their expected value only if the system is off criticality. However, the very fact that the system is assumed to be in the critical regime implies that fluctuations have a dominant role in the determination of the properties of the dynamical system. In Fig. 2, for example, we display time series representative for the critical regime of the dynamics. Ground-truth time series are obtained by simulating the SIR stochastic dynamics (see Appendix for details). They are compared with the deterministic expectation value obtained by integrating Eqs. (1). We note that some realizations of the process are more persistent and more pervasive in the population than what predicted by the expected value.

From here on, we abandon the deterministic SIR equations and we embrace a stochastic approach. Critical SIR dynamics starting from a single initial seed, i.e., $n_0 = 1$, is known to be characterized by extremely large fluctuations of the outbreak size and duration. These fluctuations can be quantified by leveraging the mapping between critical SIR in a well-mixed population and the mean-field branching process. In the

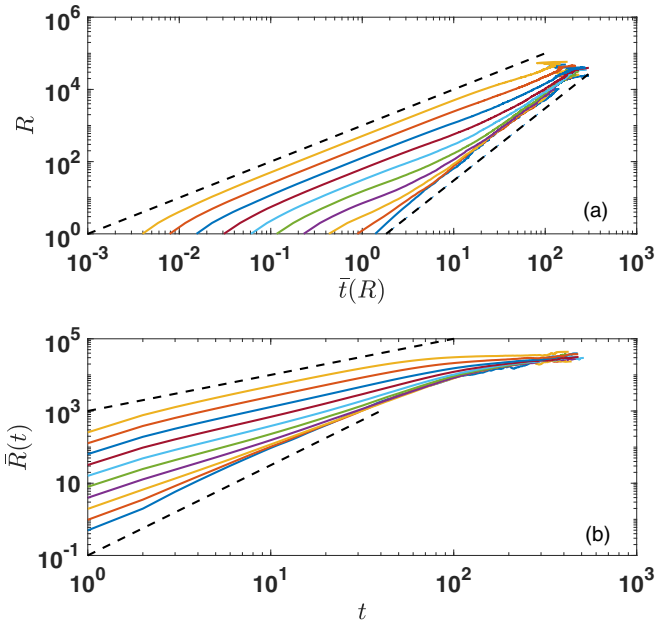

FIG. 3. Dynamical properties of the critical SIR process with nontrivial initial condition. (a) We plot the number of removed individuals R versus the expected time $\bar{t}(R)$ required to observe R removed individuals. The different curves indicate different initial conditions, from bottom to top, $n_0 = 2^q$, with $q = 2, 3, 4, \ldots, 8, 9$. The population size is $N = 10^7$. The dashed lines are guides to the eye and correspond to linear and quadratic growth of R versus $\bar{t}(R)$, respectively. (b) Expected number $\bar{R}(t)$ of removed individuals as a function of time t. Data are the same as in (a). The dashed lines are guides to the eye and correspond to power-law growth of $\bar{R}$ versus t with exponents $\xi = 1$ and 2.5, respectively.

following sections, we first review results valid for $n_0 = 1$. Then, we focus our attention on the nontrivial case $n_0 > 1$.

A. Critical dynamics with $n_0 = 1$ initial seed

If the initial condition is such that only one node is in the infected state while all other nodes are in the susceptible state, the critical SIR model gives rise to outbreaks that follow the statistics of a critical branching process [36,37] corrected by some scaling functions $F_T(N/N_T^\star)$ and $F_R(N/N_R^\star)$ that implement the effective cutoff caused by finite-size effects [33,34]. Here, N is the size of the system; $N_T^\star$ and $N_R^\star$ are instead parameters that determine when the cutoff takes place. Specifically, the distribution $P(T)$ of the duration T of an outbreak follows the law

$$P(T) \sim T^{-2} F_T(N/N_T^\star), \tag{16}$$

while the size of the outbreak R follows the distribution

$$P(R) \sim R^{-3/2} F_R(N/N_R^\star). \tag{17}$$

The cutoff sizes $N_T^\star$ and $N_R^\star$ have been derived in Refs. [33,34]. They are given by

$$N_T^\star = T^3, \quad N_R^\star = R^{3/2}. \tag{18}$$

From the expressions for $P(T)$ and $P(R)$ given by Eqs. (16) and (17), respectively, and further assuming a sharp cutoff, it is easy to deduce that the scaling with the system size N of the average outbreak size $\langle R \rangle$, the average duration $\langle T \rangle$, and the standard deviations σ_R and σ_T [33,34] obey

$$\begin{aligned} \langle R \rangle &\sim N^{1/3}, \quad \sigma_R \sim N^{1/2}, \\ \langle T \rangle &\sim \ln N, \quad \sigma_T \sim N^{1/6}. \end{aligned} \tag{19}$$

We observe that all the above quantities are subextensive, as they all grow sublinearly with the system size. The expected critical outbreak size $\langle R \rangle$ grows as the system size to the power of $\frac{1}{3}$. However, the standard deviation associated to the outbreak size, i.e., σ_R, grows with increasing system size much faster than $\langle R \rangle$. This fact indicates that it is very challenging to make predictions if the dynamics is critical. Similarly, the outbreak duration is characterized by large fluctuations in the large population limit. We note that the exponents 2 and $\frac{3}{2}$ of the distribution $P(T)$ and $P(R)$ are the critical mean-field exponents. These exponents are universal and are observed for many critical spreading processes [41]. They characterize the critical SIR on network topologies too as long as the underlying network has a homogeneous degree distribution. In power-law networks, these exponents can deviate from their mean-field values as investigated in Refs. [41,42].

We have seen in Sec. II that the deterministic approach predicts a linear increase of the number of removed individuals with time for small time. However, such a prediction is not accurate for the ground-truth dynamics; accounting for stochastic effects correctly predicts a quadratic growth of the number of removed individuals in time when the epidemic starts with a single initial seed. To this end, the number of removed individuals grows in time as a power law

$$R = \bar{t}^z, \tag{20}$$

where z is a dynamical critical exponent, and $\bar{t}$ is the expectation value of the time necessary to observe R removed individuals. The value of the dynamical critical exponent can be obtained in different ways [37]. Here, we present the derivation of the value of the dynamical exponent based on Langevin-type equations for the dynamics. Starting from an initial fraction of infected individuals $i(0) = n_0/N$ and a fraction $r(0) = 0$ of removed individuals we write

$$\begin{aligned} \frac{di}{dt} &= (\lambda s - 1) i + c\sqrt{i}\eta(t), \\ \frac{dr}{dt} &= i, \end{aligned} \tag{21}$$

where $\eta(t)$ is an uncorrelated white noise with $\mathbb{E}(\eta(t)) = 0$ and $\mathbb{E}(\eta(t)\eta(t')) = \delta(t - t')$ and c is a constant. At criticality, i.e., $\lambda = \lambda_c = 1$, thus, assuming $t \ll 1$ and $i(0) \ll 1$, we have $\lambda s - 1 \simeq -i(0)$. We can therefore write

$$\begin{aligned} \frac{di}{dt} &= c\sqrt{i}\eta(t), \\ \frac{dr}{dt} &= i. \end{aligned} \tag{22}$$

We now perform a simple scaling analysis of this stochastic equations as usually done in nonequilibrium statistical mechanics, e.g., Refs. [38,43,44]. If we rescale time as

$$t \to bt \tag{23}$$

and define the scaling exponents z, α, for r, i

$$r \to b^z t, \tag{24}$$

$$i \to b^\alpha t, \tag{25}$$

as the exponents that leave the SIR critical dynamics unchanged. The SIR stochastic equations (22) read as

$$\begin{aligned} b^{\alpha-1}\frac{di}{dt} &= cb^{\alpha/2-1/2}\eta(t), \\ b^{z-1}\frac{dr}{dt} &= b^\alpha i, \end{aligned} \tag{26}$$

from which we can derive the scaling exponents

$$\alpha = 1, \tag{27}$$

$$z = 2. \tag{28}$$

In summary, in the critical dynamical regime, if the spreading is started from a single initial seed, we expect that the average number of removed individuals grows quadratically with time.

B. Critical dynamics with $n_0 > 1$ initial seeds

Critical SIR dynamics started from the nontrivial initial condition $n_0 > 1$ differs from the critical SIR dynamics started from $n_0 = 1$ seed. To include an explicit dependence on the parameter n_0 in the scaling of Eq. (20), we correct it by introducing the scaling function $F(x)$, where $x = n_0/\bar{t}(R)$. We impose that

$$R \simeq \bar{t}(R)^z F\left(\frac{n_0}{\bar{t}(R)}\right) \tag{29}$$

with

$$F(u) \sim \begin{cases} 1 & \text{if} \quad u \gg 1, \\ u^\beta & \text{if} \quad u \ll 1. \end{cases} \tag{30}$$

According to the deterministic SIR equations for $t \ll 1$ and $i(0) \ll 1$, the number of removed individuals grows linearly in time with a slope $i(0) = n_0/N$. Thus, we deduce that

$$\beta = 1. \tag{31}$$

This value is well supported by extensive numerical results (see Fig. 3) which confirm that there is a crossover between linear and quadratic dependence of R on $\bar{t}(R)$.

In the simulation of the SIR model, it is natural to study the behavior of R as a function of $\bar{t}(R)$. However, in real epidemic time series, the number of infected individuals is measured over constant time intervals. The two ways of monitoring the evolution of the process, i.e., R versus $\bar{t}(R)$ rather than $\bar{R}(t)$ versus time t, may lead to the observation of different scaling exponents. The discrepancy is due to the stochastic nature of the spreading process. The phenomenon is apparent from the results of Fig. 3: depending on the type of measurement performed on the system, the power-law increase of the number of removed individuals as a function of time can be described by a continuous range of exponents ranging from $\xi = 1$ to $\xi \sim 2.5$. We can therefore write

$$\bar{R}(t) \simeq n_0 t^\xi h(t, N), \tag{32}$$

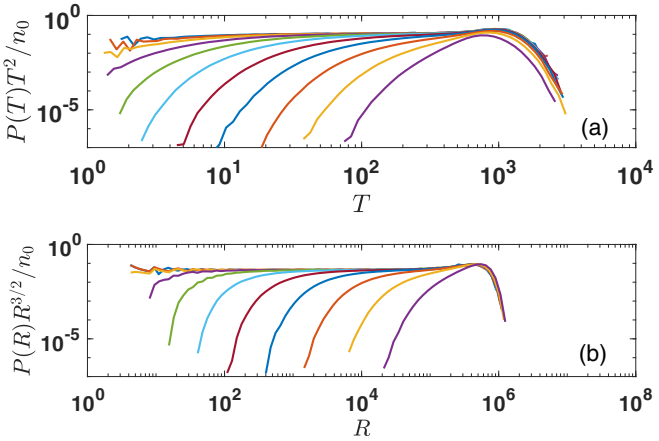

FIG. 4. The rescaled distribution of outbreak duration $P(T)$ (a) and outbreak size $P(R)$ (b) are plotted for a well-mixed population of $N = 10^8$ individuals and initial number of infected individuals n_0 equal to 2^q, with $q = 2, 3, 4, \ldots, 10, 11$. The distributions display a lower cutoff that increases as n_0 increases, and an upper cutoff whose value does not strongly depend on n_0.

where ξ is a decreasing function of n_0, and $h(t, N)$ is a modulating function expressing the deviation from the pure power-law behavior. The ansatz of the above equation is compatible with the power-law scaling of the empirical time series of removed individuals as a function of time observed in countries where containment measures have been implemented extensively [12,14,16,17].

C. Distribution of avalanche durations and sizes for the critical SIR model initiated by $n_0 > 1$ seeds

In this section we investigate the statistical properties of the distribution of outbreak duration and size for the critical SIR dynamics in a well-mixed population when the initial condition is nontrivial, i.e., $n_0 > 1$. Scaling arguments suggest the following expression for the distribution $P(T)$ of the critical outbreak duration T:

$$P(T) \sim n_0 T^{-2} F_T(N/N_T^\star, n_0/T). \tag{33}$$

The above scaling function is a natural modification of Eq. (16) by assuming that n_0 scales like time. In particular, the distribution $P(T)$ is characterized by a lower cutoff depending on n_0. This fact is intuitive as an outbreak with a larger number of initially infected individuals is not expected to reach the absorbing state faster than an outbreak started by a single seed [see Fig. 4(a)]. We note that, in the critical SIR dynamics, the dependence on n_0 does not lead to a change of the critical exponent values, as for example observed in other nonequilibrium phase transitions [38–40]. In Fig. 5(a), we display the function

$$w_T(n_0, T) = -\ln \frac{F_T(N/N_T^\star, n_0/T)}{F_T(N/N_T^\star, 1/T)} \tag{34}$$

and we demonstrate that the scaling function $w_T(n_0/T)$ for $n_0 \ll N_T^\star$ can be approximated as

$$w_T(n_0, T) \simeq -\frac{n_0 - 1}{T}. \tag{35}$$

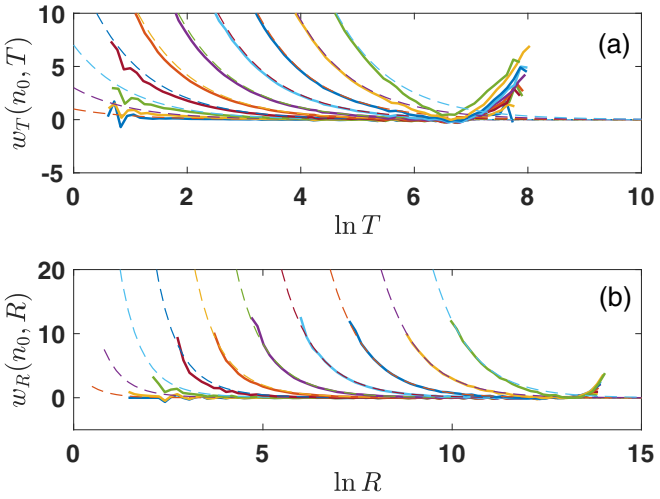

FIG. 5. The function $w_T(n_0, T)$ and $w_R(n_0, R)$ defined in Eq. (34) (a) and Eq. (39) (b) are plotted for a population of $N = 10^8$ individuals and different values of $n_0 = 2^q$, with $q = 2, 3, 4, \ldots, 10, 11$. The dashed lines correspond to the scaling expressed in Eqs. (35) and (40).

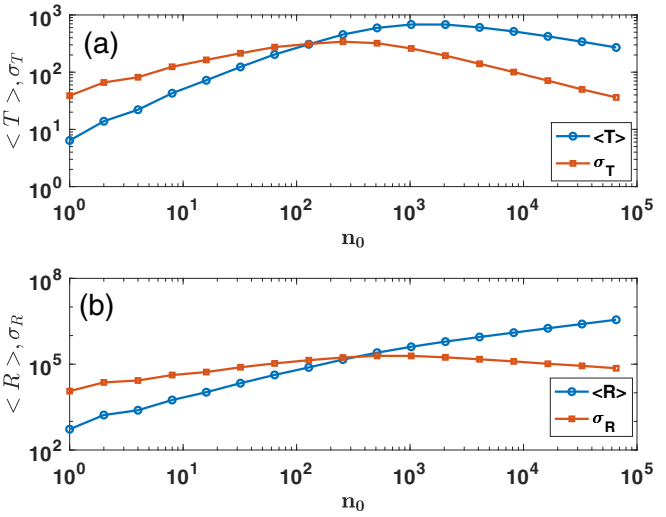

FIG. 6. (a) The expected value of the duration of critical outbreak $\langle T \rangle$ and the corresponding standard deviation σ_T are plotted versus the number n_0 of individuals initially infected. The population size is $N = 10^8$. Results are obtained relying on 10^4 independent realizations of the process. (b) The expected size of the critical outbreak $\langle R \rangle$ and the corresponding standard deviation σ_R are plotted versus the number n_0 of individuals initially infected. Data are the same as of (a).

The scaling behavior, valid for $n_0 \ll N^{1/3}$, can be justified by assuming that each of the n_0 seeds generates an independent outbreak obeying the statistics of the critical branching process. A critical avalanche started from a single infected individual has a duration T following the power-law distribution $\pi(T) \sim T^{-2}$ [36,37]. Thus, assuming independence among the n_0 avalanches, we can estimate the probability $P(T)$ as the probability that among all n_0 outbreaks the last outbreak to get extinguished is extinguished at time T. Therefore, in the infinite population limit we obtain

$$P(T) \simeq n_0[1 - \pi_c(T)]^{n_0 - 1}\pi(T), \tag{36}$$

where $\pi_c(T)$ is the probability that an outbreak generated by a single infected individual is not extinguished at time T, with $\pi_c(T) \int_T^\infty \pi(x)dx \simeq 1/T$. By assuming $1 \ll n_0 \ll N^{1/3}$, we get

$$P(T) \simeq n_0 \exp\left(-\frac{n_0 - 1}{T}\right). \tag{37}$$

Finally, we note that while the scaling behavior described in Eq. (35) has strong numerical confirmation for $T \ll N_T^\star$ for values of $T \sim N_T^\star$ the scaling function $w_T(n_0, T)$ signals a dependence of the cutoff on n_0 (see Fig. 5).

Scaling arguments suggest that the distribution $P(R)$ of critical outbreak size R should obey

$$P(R) \sim n_0 R^{-3/2} F_R(N/N_R^\star, n_0, R), \tag{38}$$

where the function $F_R(N/N_R^\star, n_0, R)$ implements a lower cutoff dependent exponentially on n_0 [see Fig. 4(b)].

In Fig. 5(b), we show the function

$$w_R(n_0, R) = -\ln \frac{F_R(N/N_R^\star, n_0, R)}{F_R(N/N_R^\star, 1, R)} \tag{39}$$

which, for $n_0 \ll N_R^\star(R, n_0)$, can be approximated as

$$w_R(n_0, R) \simeq -\frac{n_0^2}{R} - \frac{n_0^{5/2}}{R^2}. \tag{40}$$

This scaling function indicates that, for large values of R, R scales like n_0^2. For small values of R, it is possible to observe some corrections would be required to fully describe the scaling. We notice that, in the first order in n_0, the normalization constant of the distribution $P(R)$ is independent of n_0. A way to interpret the result is by considering the infinite population limit approximating the distribution $P(R)$ as the convolution of the n_0 sizes of independent outbreak events. In this limit we have

$$P(R) = \int d\omega\, e^{i\omega R}[\mathcal{F}(\omega)]^{n_0}, \tag{41}$$

where $\mathcal{F}(\omega) = \sum_r \Pi(r)e^{-i\omega r}$ is the generating function of the distribution $\Pi(r)$ of avalanches sizes of SIR critical dynamics starting from a single seed. Assuming in first approximation that $\Pi(r)$ is a pure power law $\Pi(r) \sim r^{-3/2}$, it follows that the logarithm of the generating function behaves, for small ω, as $\ln \mathcal{F}(\omega) \sim \sqrt{\omega}$. The result, together with Eq. (41), indicates that R should scale as n_0^2 for $n_0 \ll N^{2/3}$. For more details on the infinite population limit we refer the reader to Ref. [45].

D. Statistical properties of the critical outbreak started by $n_0 > 1$ seeds

1. General scenario

We performed large-scale simulations of the critical SIR model to address fundamental questions regarding the distributions of duration T and size R of outbreaks started by a nontrivial initial condition $n_0 > 1$. In Fig. 6, we display the average values and the standard deviations of both T and R for a large system composed of $N = 10^8$ individuals. We display the moments of the distributions as a function of the number of initial seeds n_0. The main outcomes are as follows. The

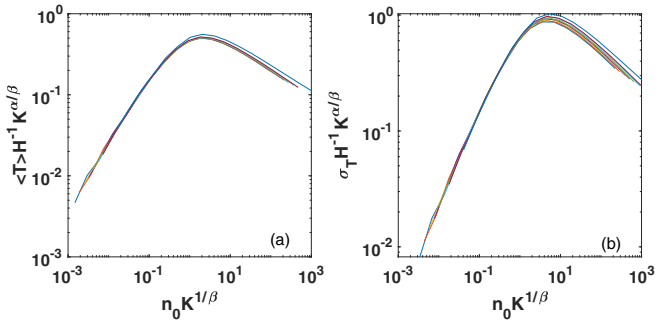

FIG. 7. Finite-size scaling analysis for the duration T of the critical SIR started from n_0 initial seeds. (a) Data describing the average value of the outbreak duration $\langle T\rangle$ for different system sizes N are collapsed on a unique universal curve using the scaling of Eq. (45). Data are shown for population sizes N ranging from $N = 10^5$ to 10^8. Each data point is obtained by simulating the SIR process 10^4 times. (b) Same as in (a), but for the standard deviation σ_T.

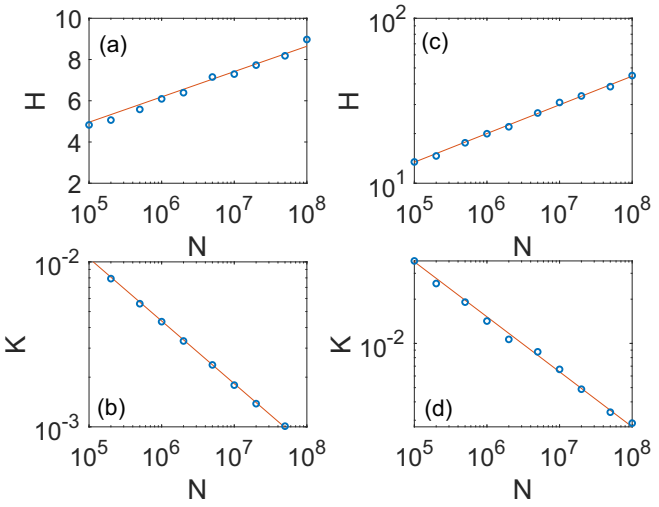

FIG. 8. (a) Scaling parameter H as a function of the system size N for the average duration $\langle T\rangle$ of critical outbreaks. Data points are the same as those of Fig. 7. The line displays the best fit of the data points with Eq. (47). (b) Same as in (a), but for the scaling parameter K. (c) Same as in (a), but for the standard deviation σ_T. The orange line is the best fit of the data points with Eq. (50). (d) Same as in (c), but for the scaling parameter K.

expected size $\langle R\rangle$ is a growing function of n_0. The expected duration $\langle T\rangle$ is a nonmonotonic function of n_0, displaying a single peak. The standard deviations σ_T and σ_R also display a peak as a function of n_0. The coefficients of variation $\sigma_T/\langle T\rangle$ and $\sigma_R/\langle R\rangle$ are monotonically decreasing with n_0. We conclude that fluctuations are fundamental to properly characterize the critical dynamical regime. This statement is true for any value of n_0, albeit, in relative terms, the most severe effect of fluctuations is observed for $n_0 = 1$. We note that as the initial number of infected individuals n_0 increases, the expected size of the outbreak displays a monotonic increase while the expected duration of the outbreak displays a maximum. In the following subsection, we will provide scaling laws for these major statistical properties of the critical dynamics as a function of the number of initially infected individuals.

2. Scaling analysis of $\langle T\rangle$ and σ_T

We make the ansatz that the average duration $\langle T\rangle$ can be described by

$$\langle T\rangle \simeq G(n_0|\alpha,\beta,H,K), \tag{42}$$

where the function $G(n_0|\alpha,\beta,H,K)$ is given by

$$G(n_0|\alpha,\beta,H,K) = \frac{n_0^\alpha H}{1+n_0^\beta K}. \tag{43}$$

Here, α and β are, in the large population limit, independent of N. On the contrary, H and K are dependent on the population size. By introducing the function

$$g(x|\alpha,\beta) = \frac{x^\alpha}{1+x^\beta}, \tag{44}$$

we observe that it is possible to rescale the curves obtained for different values of N by performing the transformation

$$H^{-1}K^{\alpha/\beta}G(n_0|\alpha,\beta,H,K) = g(n_0K^{1/\beta}|\alpha,\beta). \tag{45}$$

This expression allows us to perform a data collapse of the data obtained for $\langle T\rangle$ at different values of n_0 and different population size N [see Fig. 7(a)].

We observe that, if we start from a nontrivial initial condition n_0, the expected duration of the outbreak $\langle T\rangle$ reaches its maximum at

$$n_0^\star = \left(\frac{\alpha}{K(\beta-\alpha)}\right)^{1/\beta}. \tag{46}$$

The scaling parameters H and K obey the scaling relation

$$K \simeq a_K N^{\delta_K}, \quad H \simeq a_H \log(N) + b_H \tag{47}$$

with $a_H = 0.58 \pm 0.08$, $b_H = -2.0 \pm 0.9$, $\delta_K = -0.37 \pm 0.04$, and $a_K = 0.75 \pm 0.06$ (see Fig. 8). We note that the logarithmic scaling of H is expected from the known scaling of $\langle T\rangle$ for the SIR critical model starting from a single initial seed. The exponents α and β are given by

$$\alpha = 0.78 \pm 0.03, \quad \beta = 1.10 \pm 0.1. \tag{48}$$

The standard deviation of the outbreak duration σ_T can be described in the same exact way as $\langle T\rangle$. The ansatz

$$\sigma_T \simeq G(n_0|\alpha,\beta,H,K) \tag{49}$$

leads to the data collapse shown in Fig. 7(b). The scaling parameters H and K obey the scaling relations

$$K \simeq a_K N^{\delta_K}, \quad H \simeq a_H N^{\delta_H} \tag{50}$$

with $\delta_H = 0.17 \pm 0.01$, $b_H = 1.7 \pm 0.2$, $\delta_K = -0.36 \pm 0.03$, and $a_K = 2.3 \pm 0.7$ (see Fig. 8). We note that $\delta_H \simeq \frac{1}{6}$. Therefore, for $n_0 = 1$ the scaling reduces to the well-known scaling for the critical SIR model starting from a single initial seed. Moreover, the exponent α and β for σ_T are given by

$$\alpha = 0.50 \pm 0.05, \quad \beta = 1.0 \pm 0.1. \tag{51}$$

3. Scaling analysis of $\langle R\rangle$ and σ_R

The ansatz for $\langle R\rangle$ is slightly different from the one appearing in Eq. (43), as it includes an additional logarithmic

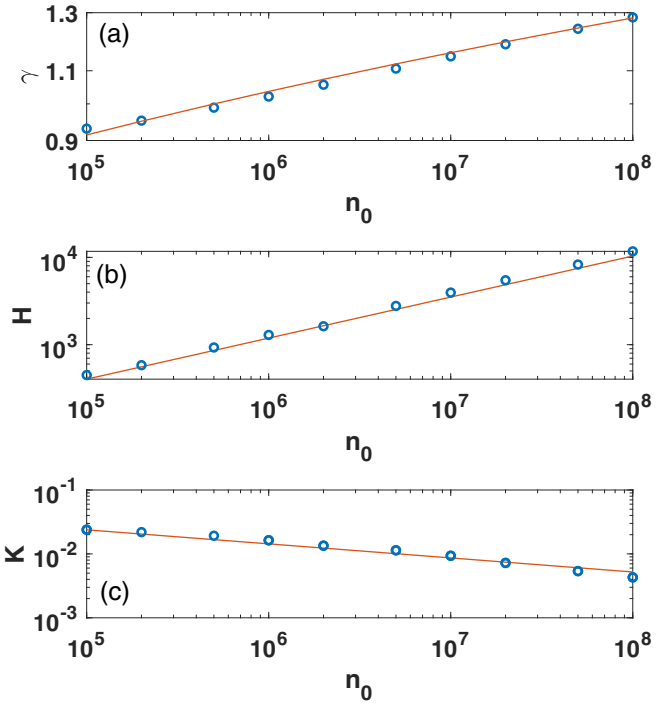

FIG. 9. (a) The fitting parameter γ, i.e., Eq. (52), as a function of the system size N. Data points are the same as those of Fig. 7. The line displays the best fit of the data points with Eq. (55). (b) Scaling parameter H as a function of the system size N for the standard deviation σ_R of critical outbreaks. The solid line corresponds to the scaling function of Eq. (60). (c) Same as in (b), but for the scaling parameter K. The solid line corresponds to the scaling function of Eq. (60).

correction

$$\langle R\rangle \simeq \frac{n_0^{\alpha} H}{1 + n_0^{\beta} (\ln n_0)^{\gamma} K}. \tag{52}$$

We take

$$H = \frac{3}{2} N^{1/3}, \quad K = N^{-1/3} \tag{53}$$

and

$$\alpha = 1, \quad \beta = 0.5 \tag{54}$$

and we perform a fit of the exponent γ. As Figs. 9(a) and 10(a) demonstrate, the function gives rise to excellent data fits as long as the exponent γ is

$$\gamma = a_{\gamma} \ln N + b_{\gamma} \tag{55}$$

with $a_{\gamma} = 0.053 \pm 0.003$ and $b_{\gamma} = 0.30 \pm 0.06$.

The function $\langle R\rangle$ can be rescaled and the data obtained for different N collapsed on a universal curve (see Fig. 10(a)). This task is done by noting that

$$\langle R\rangle y(n_0) = g(x(n_0)|\alpha, \beta), \tag{56}$$

where

$$\begin{aligned} x(n_0) &= n_0 (\ln n_0)^{\gamma/\beta} K^{1/\beta}, \\ y(n_0) &= H^{-1} K^{\alpha/\beta} (\ln n_0)^{\alpha\gamma/\beta}, \end{aligned} \tag{57}$$

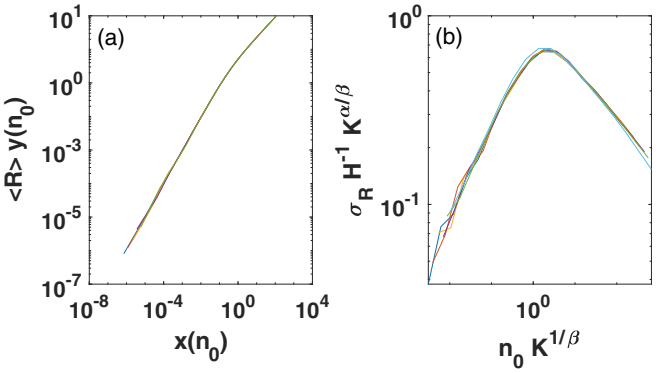

FIG. 10. Finite-size scaling analysis for the size R of the critical SIR started from n_0 initial seeds. (a) Data describing the average value of the outbreak size $\langle R\rangle$ for different system sizes N are collapsed on a unique universal curve using the scaling of Eq. (56). Data are the same as of Fig. 7. (b) Same as in (a), but for the standard deviation σ_R.

and the function $g(x|\alpha, \beta)$ is given by Eq. (44). The expected size of the outbreak $\langle R\rangle$ does not display a maximum as a function of n_0, i.e., it is a monotonous increasing function of n_0. The standard deviation σ_R can be instead fitted using the same ansatz as σ_T, i.e.,

$$\sigma_R \simeq G(n_0|\alpha, \beta, H, K). \tag{58}$$

The best estimates of the parameters are

$$\alpha = 0.57 \pm 0.03, \quad \beta = 0.95 \pm 0.05 \tag{59}$$

and

$$K \simeq a_K N^{\delta_K}, \quad H \simeq a_H N^{\delta_H} \tag{60}$$

with $\delta_H = 0.48 \pm 0.02$, $b_H = 1.8 \pm 0.5$, $\delta_K = -0.25 \pm 0.03$, and $a_K = 0.49 \pm 0.3$ (see Fig. 9(b)–9(c)). The corresponding data collapse is shown in Fig. 10(b).

IV. CONCLUSIONS

Motivated by the current COVID-19 pandemic, we have investigated the critical properties of the susceptible-infected-removed (SIR) dynamics in well-mixed populations starting from nontrivial initial conditions consisting of $n_0 > 1$ infected individuals. Although the modeling framework oversimplifies the real-world scenario, the setting is realistic in two main respects. First, the plateauing time series observed in empirical data are compatible with the critical dynamical regime. Second, the initial condition $n_0 > 1$ is representative for a critical regime reached, thanks to effective containment measures, after that a significant community transmission already took place. We have shown that a nontrivial initial condition $n_0 > 1$ introduces another typical scale on the dynamics inducing a lower cutoff in the distributions of the duration and size of critical outbreaks. The critical dynamics is characterized by very strong fluctuations, but the presence of a nontrivial initial condition mitigates the role of the fluctuations. In particular, while for a single initial seed the standard deviation on the outbreak size and duration is much larger than the corresponding expectation values, the relative error diminishes as the size n_0 of the initial seed set increases. Moreover, numerical results

indicate that, as the initial number of infected individuals n_0 increases, the expected size of the outbreak increases while the expected duration first increases and then decreases, displaying a maximum. Using scaling arguments and extensive numerical simulations we have deduced the scaling of the maximum duration and the corresponding number of initially infected individuals.

ACKNOWLEDGMENTS

We thank P. L. Krapivsky, G. Odor, and R. M. Ziff for interesting discussions. F.R. acknowledges support from the National Science Foundation (Grant No. CMMI-1552487).

APPENDIX: STOCHASTIC SIR DYNAMICS ON WELL-MIXED POPULATIONS

The critical SIR dynamics in a well-mixed population of N individuals is simulated with the following implementation of the Gillespie algorithm [46]. We indicate with $S(t)$, $I(t)$, and $R(t)$, respectively, the number of susceptible, infected, and removed individuals as a function of time t. We start from the initial condition of $I(0) = n_0$, $S(0) = N - n_0$, and $R(0) = 0$. At each elementary step, the algorithm proceeds as follows:

(i) Time increases by the amount Δt

$$t \to t + \Delta t, \tag{A1}$$

where Δt is given by

$$\Delta t = \frac{-\log(q)}{\lambda S(t) I(t) + I(t)} \tag{A2}$$

with $q \sim$ Unif.(0,1), i.e., a random variate extracted from the uniform distribution in the domain (0, 1).

(ii) With probability

$$p = \frac{\lambda S(t) I(t)}{\lambda S(t) I(t) + I(t)} \tag{A3}$$

a susceptible individual becomes infected, i.e.,

$$\begin{aligned} S(t + \Delta t) &= S(t) - 1, \\ I(t + \Delta t) &= I(t) + 1. \end{aligned} \tag{A4}$$

(iii) With probability $1 - p$ an infected individual is removed, i.e.,

$$\begin{aligned} I(t + \Delta t) &= I(t) - 1, \\ R(t + \Delta t) &= R(t) + 1. \end{aligned} \tag{A5}$$

The critical dynamics is obtained by setting $\lambda = 1$. The steps of the algorithms are iterated until the number of infected individuals is zero. This happens at time T, i.e., the duration of the outbreak. The size of the outbreak is given by $R(T)$.

[1] R. M. Anderson, B. Anderson, and R. M. May, *Infectious Diseases of Humans: Dynamics and Control* (Oxford University Press, Oxford, 1992).
[2] S. Maslov and N. Goldenfeld, arXiv:2003.09564.
[3] G. N. Wong, Z. J. Weiner, A. V. Tkachenko, A. Elbanna, S. Maslov, and N. Goldenfeld, arXiv:2006.02036.
[4] L. Ferretti, C. Wymant, M. Kendall, L. Zhao, A. Nurtay, D. G. Bonsall, and C. Fraser, Science **368**, eabb6936 (2020).
[5] G. Bianconi, H. Sun, G. Rapisardi, and A. Arenas, arXiv:2007.05277.
[6] D. Fanelli and F. Piazza, Chaos, Solitons Fractals **134**, 109761 (2020).
[7] T. Carletti, D. Fanelli, and F. Piazza, arXiv:2005.11085.
[8] A. Bianconi, A. Marcelli, G. Campi, and A. Perali, Phys. Biol. **17**, 065006 (2020).
[9] S. Bradde, B. Cerruti, and J.-P. Bouchaud, arXiv:2006.09829.
[10] P. Maheshwari and R. Albert, arXiv:2006.09189.
[11] A. Arenas, W. Cota, J. Gomez-Gardenes, S. Gómez, C. Granell, J. T. Matamalas, D. Soriano-Panos, and B. Steinegger (unpublished).
[12] A. L. Ziff and R. M. Ziff, medRxiv: 2020.02.16.20023820.
[13] G. Bianconi and P. L. Krapivsky, Phys. Rev. E **102**, 032305 (2020).
[14] M. Nekovee, medRxiv: 2020.05.18.20105445.
[15] O. Valba, V. Avetisov, A. Gorsky, and S. Nechaev, Phys. Rev. E **102**, 010401(R) (2020).
[16] B. Blasius, Chaos **30**, 093123 (2020).
[17] A. Brandenburg, Infectious Disease Model. **5**, 681 (2020).
[18] J. D. Murray, *Mathematical Biology: I. An Introduction*, Vol. 17 (Springer, New York, 2007).
[19] P. L. Krapivsky, S. Redner, and E. Ben-Naim, *A Kinetic View of Statistical Physics* (Cambridge University Press, Cambridge, 2010).
[20] A.-L. Barabási *et al.*, *Network Science* (Cambridge University Press, Cambridge, 2016).
[21] M. Newman, *Networks* (Oxford University Press, Oxford, 2010).
[22] G. Bianconi, *Multilayer Networks: Structure and Function* (Oxford University Press, Oxford, 2018).
[23] A. Barrat, M. Barthelemy, and A. Vespignani, *Dynamical Processes on Complex Networks* (Cambridge University Press, Cambridge, 2008).
[24] S. N. Dorogovtsev, *Lectures on Complex Networks*, Vol. 24 (Oxford University Press, Oxford, 2010).
[25] R. Pastor-Satorras, C. Castellano, P. Van Mieghem, and A. Vespignani, Rev. Mod. Phys. **87**, 925 (2015).
[26] M. A. Porter and J. P. Gleeson, *Dynamical Systems on Networks:A Tutorial*, Frontiers in Applied Dynamical Systems: Reviews and Tutorials Vol. 4 (Springer, Cham, Switzerland, 2016).
[27] M. Nanni, G. Andrienko, C. Boldrini, F. Bonchi, C. Cattuto, F. Chiaromonte, G. Comandé, M. Conti, M. Coté, F. Dignum *et al.*, arXiv:2004.05222.

[28] T. Gross, C. J. D. D'Lima, and B. Blasius, Phys. Rev. Lett. **96**, 208701 (2006).
[29] T. Gross and H. Sayama, *Adaptive Networks* (Springer, Berlin, 2009), pp. 1–8.
[30] T. Mora and W. Bialek, J. Stat. Phys. **144**, 268 (2011).
[31] M. A. Munoz, Rev. Mod. Phys. **90**, 031001 (2018).
[32] J. P. Gleeson and R. Durrett, Nat. Commun. **8**, 1 (2017).
[33] E. Ben-Naim and P. L. Krapivsky, Phys. Rev. E **69**, 050901(R) (2004).
[34] E. Ben-Naim and P. Krapivsky, Eur. Phys. J. B **85**, 145 (2012).
[35] T. Tomé and R. M. Ziff, Phys. Rev. E **82**, 051921 (2010).
[36] S. Zapperi, K. B. Lauritsen, and H. E. Stanley, Phys. Rev. Lett. **75**, 4071 (1995).
[37] K. B. Lauritsen, S. Zapperi, and H. E. Stanley, Phys. Rev. E **54**, 2483 (1996).
[38] M. Henkel, H. Hinrichsen, and S. Lübeck, *Non-equilibrium Phase Transitions: Absorbing Phase Transitions*, Vol. 1 (Springer, Berlin, 2008).
[39] H. Janssen, B. Schaub, and B. Schmittmann, Z. Phys. B **73**, 539 (1989).
[40] H. Hinrichsen and G. Ódor, Phys. Rev. E **58**, 311 (1998).
[41] F. Radicchi, C. Castellano, A. Flammini, M. A. Muñoz, and D. Notarmuzi, Phys. Rev. Res. **2**, 033171 (2020).
[42] K.-I. Goh, D.-S. Lee, B. Kahng, and D. Kim, Phys. Rev. Lett. **91**, 148701 (2003).
[43] A.-L. Barabási and H. E. Stanley, *Fractal Concepts in Surface Growth* (Cambridge University Press, Cambridge, 1995).
[44] J. Marro and R. Dickman, *Nonequilibrium phase transitions in lattice models* (Cambridge University Press, Cambridge, 2005).
[45] P. Krapivsky, arXiv:2009.08940.
[46] D. T. Gillespie, J. Comput. Phys. **22**, 403 (1976).